2016 CMBEC39 Conference
Calgary AB
May 24–27, 2016

# A SALIENCY-BASED UNSUPERVISED METHOD FOR ANGIOECTASIA DETECTION IN CAPSULE ENDOSCOPIC IMAGES

Farah Deeba, Shahed K. Mohammed, Francis M. Bui, Khan A. Wahid (*Authors*)
*Department of Electrical and Computer Engineering,*
*University of Saskatchewan*

## INTRODUCTION

Small intestinal bleeding presents a unique and challenging clinical problem, requiring more diagnostic procedures, more blood transfusions, longer hospitalizations and higher health care expenditures than the upper or lower GI bleeding, which is a direct consequence of inaccessibility of small bowel by traditional endoscopy [1]. Small bowel bleeding constitutes 75% of obscure gastrointestinal bleeding (OGIB) cases among which 30-40% cases are originated from angioectasias lesions [2]. Angioectasias, also known as angiodysplasias in the literature, are vascular malformations, which can be found in up to 3% of the population [3]. Small bowel capsule endoscopy (SBCE), with its ability to visualize small bowel, has become a particularly useful tool in the detection and management of angioectasias.

The potential of capsule endoscopy to examine the small intestine is downplayed by the burden of reviewing 14400-72000 CE frames per patient by the clinician [4]. Thus, development of computer-aided screening and decision making systems for abnormality detection in capsule endoscopic images have drawn much attention of researchers in recent years [5]. These researches have been conducted by classifying the abnormalities into broader categories, for example, bleeding, lesions, ulcer etc. A more useful approach could be adopted by emphasizing on the development of computer aided detection (CAD) system for specific pathologies. For example, angioectasias, the primary suspected lesion in patients with OGIB, are associated with certain clinical conditions and syndromes including aging, hemodialysis, heart failure, aortic stenosis (Heyde's syndrome), radiation therapy, and von Willebrand's syndrome [6]. In such cases, employing a CAD system particularly designed to detect angioectasias is more logical and expected to achieve better result than the system for the detection of lesions in general. Keeping this fact in mind, we have proposed a saliency based unsupervised method specifically designed for angioectasias detection.

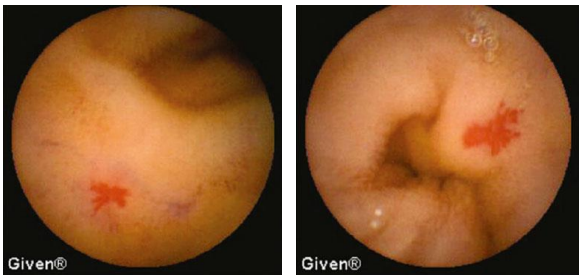

Figure 1. Example images of angioectasia lesions. Dilation of mucosa capillaries causes a reticular or

Angioectasia is characterized by flat or slightly elevated, discrete, red, fan-shaped area with delicate, reticular pattern on a background of normal small intestinal mucosa [15], as can be seen in fig. 1. From the special appearance of angioectasia lesions, they can qualify as visually salient regions in an endoscopic video frame. To utilize this characteristics, we propose a saliency based unsupervised method for angioectasias detection. In recent years, saliency algorithms have attracted attention of researchers, which extract the most informative regions from the image. In [7], a point saliency based method has been proposed to detect lesions including angioectasias, where accuracy ranging from 69.9%-97.5% has been achieved. However, this method is designed for a broad spectrum of lesions. Besides, a few works based on saliency have been published in the field of video endoscopy to detect abnormalities, e.g., bleeding [8], [9], ulcer [10], [11], polyp [12],

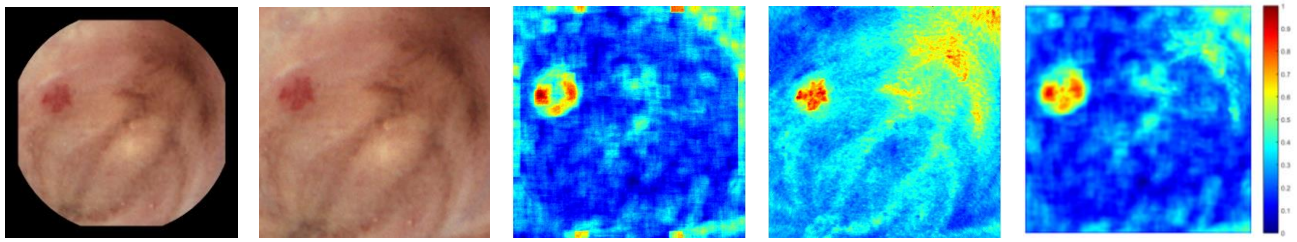

(a) (b) (c) (d) (e)

Fig. 1: A visual demonstration of first stage of the proposed methodology: (a) Original Image; (b) Image after Pre-processing; (c) PD Map; (d) Saliency map; (e) Final Saliency Map; The color bar shows the color scale applicable for (c), (d) and (e).

for video summarization [13], and for key frame extraction [14]. However, this is the first attempt to design an unsupervised algorithm based on saliency for angioectasia detection.

In this paper, we propose a two-stage unsupervised and fully automated detection algorithm. In the first stage, we construct a saliency map by combining a PD (patch distinctness) map and an IHb map obtained from endoscopic images. The PD map is formed using a distance measure which computes the distinctness of image patches compared to an average image patch [16]. The IHb map is formed using index of hemoglobin (IHb) to exploit the characterizing red hue of angioectasias. Finally, the PD map and the IHb map are combined to form the final saliency map. In the second stage, we perform a local maxima search from gradient image obtained from the saliency map to localize the ROIs (region-of-interests). The proposed method presents an efficient algorithm, which is able to detect even very small angioectasias lesions without learning any a priori information.

## FIRST STAGE: SALIENCY MAP FORMATION

### Pre-Processing

To avoid the border edges of capsule endoscopic images, we apply a radial mirroring on the image. The resulting image after mirroring has been shown in Fig. 1 (b).

### PD Map Construction

A patch that is different from all other patches is considered to be salient. Patch distinctiveness map is constructed to identify the distinctive, i.e., salient regions in the image. To compute the distinctiveness of the patches, first the image is divided into $k \times k$ overlapping image patches and the average patch is computed. Then the distance of each patch is computed from the average patch along the corresponding principal axis [16]. The resulting PD map is shown in Fig. 1(c).

### IHb Map Construction

The index of hemoglobin (IHb) can evaluate the hemoglobin content in gastrointestinal mucosa [17]. To calculate IHb for each pixel of the image, we use the following equation [18]:

$$\mathrm{IHb} = 32[\log_2(R/G)] \qquad [1]$$

Here, $R$ and $G$ are the red and green channel value of the corresponding pixel. From our experiment, we have found that angioectasias lesions are distinctively highlighted in the $IHb$ map, as is expected due to their reddish hue. However, some unwanted regions (for example, mucosal folds, lumen, etc.) are also included in highlighted regions in IHb map as can be seen in Fig. 1 (d).

### Saliency Map Construction:

Both PD map and IHb map emphasize the regions containing angioectasia, along with a few unwanted regions. We combine these two maps to form the final saliency map, $S$ :

$$S = PD \square IHb \qquad [2]$$

Here, $PD$ and $IHb$ stand for PD map and IHb map respectively, and $\square$ stands for Hadamard product. The final saliency map, after image stretching, emphasizes the regions which are highlighted both in PD map and IHb map.

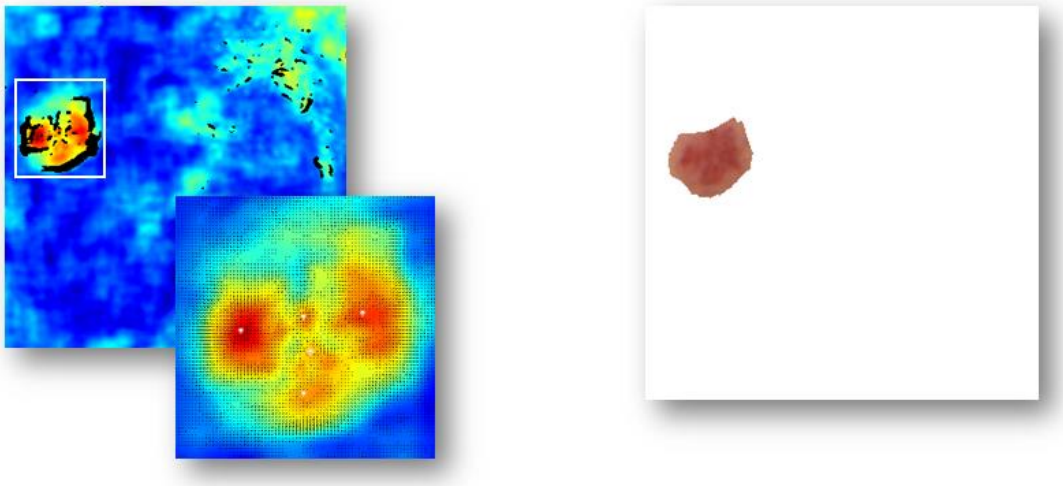

(a) (b)

Fig. 3: A demonstration of second stage of the proposed methodology: (a) Gradient Image; The ROI has been zoomed for better visualization; 5 maximum points have been detected, which act as the centers for the grown

### SECOND STAGE: ROI LOCALIZATION

In the second stage, we localize the region of interests from the final saliency map. Though a simple thresholding could extract the regions partially, a closer look into the gradient image obtained from the saliency map reveals a distinct pattern of gradient vectors toward the center of ROIs (Fig. 3(a)). From the gradient image, we extract all the maximum points (associated with gradient zero), with saliency value greater than a threshold, $T_{max}$. Then, these maximum points act as seeds for region growing. Merging the resulting regions gives the final image, as can be seen in Fig 3(b).

## EXLPERIMENTAL RESULTS

Data Description

We created a dataset containing 50 normal images and 50 images containing angioectasia. The images containing angioectasia have a total of 107 connected regions containing angioectasias lesions and vary from pixel size 3 to pixel size up to 6,000. As it is difficult to obtain large number of images for a specific pathology, therefore we had to restrict our dataset to the number of available images for angioectasia.

Experimental Results

For evaluation of the performance of our proposed method, we used the following performance metric:

$$\text{Sensitivity} = \frac{TP}{TP+FN}$$

$$\text{Specificity} = \frac{TN}{TN+FP}$$

$$\text{Accuracy} = \frac{TP+TN}{TP+TN+FP+FN}$$

Here, TP and TN are the correctly labeled abnormal and normal instances respectively and FP and FN are incorrectly labeled abnormal and normal instances respectively. For $T_{max}=0.9$, we obtain the results, as shown in Table 1.

Table 1: Experimental Results

| Sensitivity (%) | Specificity (%) | Accuracy (%) |
|---|---|---|
| 100 | 82.5 | 90.1 |

From table 1, we can see that the proposed method can achieve a very high sensitivity, with a moderate specificity. The method is not

scale dependent, thus can detect regions with widely varying areas.

## CONCLUSION

In this paper, we propose a sophisticated and effective method for angioectasia detection. The unsupervised method is able to achieve perfect sensitivity. Moreover, it can localize the region-of-interest as is evident from Fig. 1. The utility of IHb index for angiectasia detection has been first established in this paper. IHb index can be helpful for detecting other lesions with reddish hue. In our experiment, we find that uninformative image parts, for example, mucosal fold, lumen, and intestinal waste are also detected as salient region and thereby result in poor specificity. In our future research, we intend to perform pre-processing on CE images to remove these uninformative image regions beforehand. The proposed method can further be extended to detect another pathologies by incorporating characteristic color or texture information in place of IHb index, which we intend to investigate in our future research.

## REFERENCES


[1] E. J. Carey and D. E. Fleischer, "Investigation of the small bowel in gastrointestinal bleeding--enteroscopy and capsule endoscopy.," *Gastroenterol. Clin. North Am.*, vol. 34, no. 4, pp. 719–34, 2005.

[2] T. Cúrdia Gonçalves, J. Magalhães, P. Boal Carvalho, M. J. Moreira, B. Rosa, and J. Cotter, "Is it possible to predict the presence of intestinal angioectasias?," *Diagn. Ther. Endosc.*, vol. 2014, 2014.

[3] C. M. Höög, O. Broström, T. L. Lindahl, A. Hillarp, G. Lärfars, and U. Sjöqvist, "Bleeding from gastrointestinal angioectasias is not related to bleeding disorders - a case control study.," *BMC Gastroenterol.*, vol. 10, p. 113, 2010.

[4] A. Koulaouzidis, E. Rondonotti, and A. Karargyris, "Small-bowel capsule endoscopy: A ten-point contemporary review," *World J. Gastroenterol.*, vol. 19, no. 24, pp. 3726–3746, 2013.

[5] D. K. Iakovidis and A. Koulaouzidis, "Software for enhanced video capsule endoscopy: challenges for essential progress," *Nat. Rev. Gastroenterol. Hepatol.*, vol. 12, no. 3, pp. 172–186, 2015.

[6] M. Keuchel, F. Hagenmüller, and H. Tajiri, *Video capsule endoscopy: A Reference Guide and Atlas*. Springer, 2015.

[7] D. K. Iakovidis and A. Koulaouzidis, "Automatic lesion detection in capsule endoscopy based on color saliency: Closer to an essential adjunct for reviewing software," *Gastrointest. Endosc.*, vol. 80, no. 5, pp. 877–883, 2014.

[8] Y. Yuan, B. Li, and Q. Meng, "Bleeding Frame and Region Detection in the Wireless Capsule Endoscopy Video," *IEEE J. Biomed. Heal. Informatics*, vol. 2194, no. c, pp. 1–1, 2015.

[9] D. K. Iakovidis, S. Member, D. Chatzis, and P. Chrysanthopoulos, "Blood Detection in Wireless Capsule Endoscope Images based on Salient Superpixels," in *Engineering in Medicine and Biology Society (EMBC),* no. 1, pp. 731–734, 2015,.

[10] Y. Chen and J. Lee, "Ulcer Detection in Wireless Capsule Endoscopy Video," *Proc. 20th ACM Int. Conf. Multimed.*, pp. 1181–84, 2012.

[11] Y. Yuan, J. Wang, B. Li, and M. Meng, "Saliency based Ulcer Detection for Wireless Capsule Endoscopy Diagnosis," *IEEE Trans. Med. Imaging*, vol. 0062, no. c, pp. 1–1, 2015.

[12] Y. Yuan and M. Q. H. Meng, "Polyp classification based on Bag of Features and saliency in wireless capsule endoscopy," *Proc. - IEEE Int. Conf. Robot. Autom.*, pp. 3930–3935, 2014.

[13] I. Mehmood, M. Sajjad, and S. W. Baik, "Video summarization based tele-endoscopy: A service to efficiently manage visual data generated during wireless capsule endoscopy procedure," *J. Med. Syst.*, vol. 38, no. 9, 2014.

[14] Y. Yuan and M. Q.-H. Meng, "Hierarchical key frame extraction for wireless capsule endoscopy video based on the saliency map," *Int. J. Mechatronics Autom.*, vol. 4, no. 4, pp. 259–268., 2014.

[15] D. L. Stockman, *Diagnostic Pathology: Vascular*. Elsevier, 2016.

[16] L. Z.-M. Margolin, Ran, Ayellet Tal, "What Makes a Patch Distinct?," in *Proceedings of the IEEE Conference on Computer Vision and Pattern Recognition*, 2013, p. 2.

[17] W.-C. Cheng, H.-C. Cheng, P.-J. Chen, J.-W. Kang, E.-H. Yang, B.-S. Sheu, and W.-Y. Chen, "Higher net change of index of hemoglobin values between colon polyp and nonpolyp mucosa correlates with the presence of an advanced colon adenoma," *Adv. Dig. Med.*, pp. 1–6, 2015.

[18] H. K. Gwang, B. K. Kwang, K. L. Eun, H. C. Seong, O. K. Tae, J. Heo, H. K. Dae, A. S. Geun, M. Cho, and Y. P. Do, "Analysis of endoscopic electronic image of intramucosal gastric carcinoma using a software program for calculating hemoglobin index," *J. Korean Med. Sci.*, vol. 21, no. 6, pp. 1041–1047, 2006.